Angewandte Chemie
Eine Zeitschrift der Gesellschaft Deutscher Chemiker

Supporting Information

Reversibly photoswitching upconversion nanoparticles for super-sensitive photoacoustic molecular imaging

Cheng Liu,[+[a]] Xianchuang Zheng,[+[a]] Tingting Dai,[a] Huiliang Wang,[c] Xian Chen,[d] Bing Chen,[d] Tianying Sun,[d] Feng Wang,[d] Steven Chu,[b] Jianghong Rao*[a]

[+] These authors contributed equally to this work.

Table of Contents

Experimental Procedures

Materials. All chemicals were purchased from Millipore Sigma unless otherwise stated. The $NaYF_4$/Yb/Tm (59/1 %) UCNP core and $NaYF_4$/Yb/Tm (59/1 %) @$NaYF_4$ core/shell UCNP were synthesized according to the previous work.[1]

General instrument. The TEM images were collected on a JEOL JEM-1400 Transmission Electron Microscope. The emission spectra of the UCNPs were measured on a Horiba Jobin Yvon FluoroMax-3 spectrofluorometer equipped with a CW 980 nm laser (3 W, beam diameter 1 mm, LSR-PS-II, Lasever Inc.). The lifetime of the nanoprobe was acquired on an Edinburgh FLSP980 spectrometer equipped with a 980 nm pulsed laser. The absorption spectra were measured on an Agilent Cary 8453 UV-Visible Spectrophotometer. The nanoprobe's hydrodynamic diameter and zeta potential distribution were measured on a Zetasizer Nano ZS90 dynamic light scattering (DLS) analyzer (Malvern Instruments). The Yttrium (Y) concentration was measured on a high-resolution inductively coupled plasma mass spectrometer (ICP-MS, NU ATTOM). The fluorescence images of the cells were collected on a Zeiss LSM 880 laser scanning confocal microscope. The photoacoustic (PA) imaging was performed on a Nexus 128 *in vivo* PA imaging system (Endra Life Science) with an additional CW 980 nm laser (3 W, beam diameter 1 mm, LSR-PS-II, Lasever Inc.) for photoswitching through raster scanning. The average power density of the scan area (1 cm^2) was estimated to be 3 W/cm^2.

PA imaging system. The geometry of the detection system consists of 128 unfocused transducers (center frequency 5 MHz, bandwidth about 70%) arranged on a

hemispherical bowl (radius 101 mm). The bowl is filled with water, with the temperature maintained at 38 ºC. A transparent plastic tray is placed above the hemispherical bowl for holding the phantoms or animals. An Nd: YAG laser (tunable in 680 to 950 nm, pulse width 7 ns, OPOTEK Inc., USA) is used for excitation, and the laser light is delivered from the bottom of the bowl. The laser power delivered on the samples was measured to be approximately 3 to 6 mJ per pulse, depending on the wavelengths. The water temperature and laser power are real-time measured and recorded in a log file for reference. For animal imaging, the mice are anesthetized with 3% isoflurane in oxygen in the introduction chamber and then transferred to the plastic tray with 1.5% isoflurane in oxygen to maintain anesthesia.

The PA imaging systems provide a “Step and Shoot” mode for the scan, in which the bowl is rotated in steps through 120 – 180 positions in a single scan. At each position, the signals are collected with multiple laser pulses to obtain an average result. With a 20 Hz repetition rate of the laser, 120 rotation positions, and 10 pulses per position, the PA signals upon the excitation with 1,200 laser pulses will be collected in 1 min. Due to the extra self-preparation time of the system (0.9 min), in total, it will take 1.9 min to finish a scan for a single excitation wavelength. This frame rate can be adjusted by changing the number of rotation positions or pulses per position. The images are reconstructed in volumes of 256×256×256 with the voxel size of 0.1×0.1×0.1 mm^3 using a filtered back-projection algorithm. A detailed description of the reconstruction algorithm can be found in the literature.[2] In our study, the PA images are presented as maximum intensity projections (MIP). The number of slices for projection is 128, and the thickness of each slice is 100 μm.

This PA imaging system has an isotropic spatial resolution of 100 μm and an imaging depth of up to 3.5 cm as determined in tissue-mimicking phantoms.[3,4]

Synthesis of the photoswitchable small molecule.

Synthesis of 1-[4,5-Bis(2,5-dimethylthiophen-3-yl)thiophene-2-yl]ethanone. This compound was synthesized using a modified method based on the literature procedure.[5] Briefly, a mixture of 1-(4,5-dibromothiophen-2-yl)ethanone (95 mg, 0.33 mmol), 2,5-dimethylthien-3-yl boronic acid (125 mg, 0.8 mmol), tetrakis(triphenylphosphane)palladium (23 mg, 0.02 mmol) and potassium carbonate (185 mg, 1.33 mmol) was added with 1,4-dioxane (5 mL) and distilled water (0.67 mL), and then refluxed overnight at 110 ºC under Ar protection. After reaction, the mixture was cooled to room temperature, extracted with dichloromethane, washed with brine, dried over anhydrous magnesium sulfate before purified by column chromatography (Eluent: dichloromethane/n-hexane = 1:4 to pure dichloromethane). The pure compound was obtained as a light yellow solid (Yield: 90 %). ^{1}H NMR (300 MHz, $CDCl_3$): δ 7.60 (s, 1 H), 6.43-6.45 (d, 2 H), 2.56 (s, 3H), 2.36-2.38 (d, 6H), 2.07 (s, 3H), 2.00 (s, 3H); LC-MS: calculated for $C_{18}H_{18}OS_3$: 346; found: 347 $[M + H]^+$.

Synthesis of 1-(4,5-bis(2,5-dimethylthien-3-yl)thiophen-2-yl)butane-1,3-dione. 3ThacacH was synthesized using a different method with the literature procedure.[30] 1-[4,5-Bis(2,5-dimethylthiophen-3-yl)thiophene-2-yl]ethanone as synthesized above (14 mg, 0.04 mmol) in dry ethyl acetate (1.5 mL) was dropwise added to sodium amide (8 mg, 0.2 mmol) suspended in dry ethyl acetate (1.5 mL) at 0 ºC. The mixture was stirred for 1 h at 0 ºC and then refluxed overnight under Ar protection. After the reaction, the solvent was removed under vacuum. Then the mixture was quenched with HCl (1 M), extracted with chloroform, washed with brine, and dried over anhydrous magnesium sulfate before high performance liquid chromatography (HPLC). The pure compound was obtained as a light yellow solid and used as the open form of 3ThacacH (Yield: 60 %). ^{1}H NMR (300 MHz, $CDCl_3$): δ 7.63 (s, 0.17H), 7.60 (s, 0.83H), 6.46 (s,

1H), 6.42 (s, 1H), 6.00 (s, 0.83H), 4.02 (s, 0.34H), 2.37-2.38 (d, 6 H), 2.14 (s, 3H), 2.07 (s, 3H), 2.01 (s, 3H); keto/enol forms: 17/83 %; LC-MS: calculated for $C_{20}H_{20}O_2S_3$: 388; found: 389 $[M + H]^+$.

Synthesis of the photoswitchable nanoprobe. Poly(styrene-maleic anhydride) (PSMA) (average M_n ~1,900, 300 mg, 0.158 mmol), polyether amine M2070 (M_n = 2,000, 640 mg, 0.32 mmol) were dissolved in $CHCl_3$ (20 mL) into a flask equipped with a magnetic stir bar. Stir the solution at room temperature overnight to obtain the amphiphilic polymer PSMA-M2070 (45 mg mL^{-1}) in $CHCl_3$. Next, to a solution of $CHCl_3$ (3 mL) dissolving 3ThacacH small molecules (0.5 mg mL^{-1}, 100 µL, 0.05 mg) and the amphiphilic polymer (45 mg mL^{-1}, 66 µL, 3 mg) was added the $NaYF_4$/Yb/Tm (59/1 %) @$NaYF_4$ core/shell UCNPs (50 mg mL^{-1}, 10 µL) in a scintillation vial. This formulation was optimized after multiple trials. The mixture was stirred at room temperature for 2 h. Remove the $CHCl_3$ solvent completely using a rotary evaporator under reduced pressure to obtain a thin membrane on the bottom of the scintillation vial. The dry residue was dissolved in distilled water (1 mL) after sonication in a Branson 1800 ultrasonic cleaner for 15 mins. The suspension was heated to 80 ºC for 30 mins, slowly cooled down to room temperature, and sonicated for another 15 mins to obtain a clear solution.[6] Then the solution was washed with distilled water by spin-dialysis (100 kDa) and filtered by ultrafiltration (200 nm). For comparison, the nanoprobe without 3ThacacH was synthesized using the same protocol as mentioned above, except that no 3ThacacH was added in the first step.

To determine the mass concentration of the UCNP in the final nanoprobe suspension, a portion of the nanoprobe suspension was digested with concentrated nitric acid, and the concentration of Y was measured using ICP-MS. The molar

concentration (n) of the UCNP was estimated by a formula: $n = \frac{m}{\rho\frac{\pi}{6}d^3 N_A}$ where m is the mass concentration of UCNP, ρ is the density of $NaYF_4$ crystal (4.3 g mL^{-1}), d is the diameter of the UCNP, N_A is the Avogadro constant. Based on the TEM and DLS data of the nanoprobe, each nanoprobe typically contains just one UCNP, so the molar concentration of the nanoprobe equals the molar concentration of the UCNP. The mean number of 3ThacacH in each nanoprobe was estimated to be $1.4x10^4$. The calculation details are shown in Table S5.

The Förster distance (R_0) between Tm^{3+} (donor) and 3ThacacH (acceptor) in the nanoprobe was calculated using the formula: $R_0^6 = \frac{9000 ln ln\,(10)\ \kappa^2\ Q_D\ J}{128\,\pi^5\,n^4\,N_A}$, where κ^2 is dipole orientation factor (2/3 for an arbitrary orientation), Q_D is the quantum yield of the donor in the absence of acceptor, n is the refractive index of the medium (1.333 for water), and J is spectra overlap integral. The value of J was calculated using the formula: $J = \frac{\int f_D(\lambda)\,\epsilon_A(\lambda)\,\lambda^4\,d\lambda}{\int f_D(\lambda)\,d\lambda}$, where $f_D(\lambda)$ is emission intensity of the donor, and $\epsilon_A(\lambda)$ is the molar absorption coefficient of the acceptor. Based on the emission spectrum of UCNP and absorption spectrum of open form 3ThacacH (Figure 1g), the value of J was calculated to be $9.248x10^{13}$ nm^4/ (M cm). Thus, R_0 was calculated to be 3.6 nm.

Photoswitching of the mixture of UCNP and photoswitchable small molecule in $CHCl_3$. The photoswitchable small molecule 3ThacacH (open form) was added to the $CHCl_3$ suspension of UCNP (0.5 mg mL^{-1}) to the final concentration of 0.1 mM. The mixture samples in a 2 mL quartz cuvette were scanned with a 980 nm laser for 0, 1, or 2 mins before collecting their absorption spectra on an Agilent Cary 8453 UV-Visible Spectrophotometer. The 640 nm absorption peak followed the photoswitching of 3ThacacH from the open to the closed form.

Photoswitching of the nanoprobe in water. The nanoprobe was prepared in distilled water to a concentration of 2.5 nM. The absorption spectrum of the sample was first measured in the initial OFF state of the nanoprobe on an Agilent Cary 8453 UV-Visible Spectrophotometer. Then the sample in a 2 mL quartz cuvette was scanned with the 980 nm laser (3 W, beam size 1 mm) at different times (0 – 60 s) before collecting their absorption spectra. The switching ON of the nanoprobe was detected by following the broad absorption peak centered at 640 nm. Afterward, the sample was exposed to a 640 nm laser (average power density 10 mW/cm^2) for 10 s to measure their absorption spectra. The switching OFF of the nanoprobe was monitored by the gradual decrease of the 640 nm absorption peak.

Photoswitching of the PA signal of the nanoprobe in tube phantoms. PA imaging of the aqueous suspension of the nanoprobe (5 nM, 100 µL) in a transparent plastic tube (material: polypropylene, wall thickness: 0.4 mm) was performed on an Endra Nexus 128 *in vivo* PA imaging system. Because the excitation wavelength in the instrument is in the range of 680 to 950 nm, 680 nm was applied to generate the PA signal since it is closest to the absorption peak of the nanoprobe in its ON state. The PA signal was first collected in the initial OFF state of the nanoprobe. Then the sample was scanned with the 980 nm laser for 1 min to switch the nanoprobe to the ON state, followed by the PA imaging at 680 nm—the ON state signal. The 680 nm pulsed laser (7 ns pulses, 3 mJ, 20 Hz) excited the nanoprobe to produce a PA signal and gradually switched the nanoprobe back to the OFF state during the PA signal collection. The cycle of switching ON, collecting PA signal/ switching OFF, and collecting PA signal was repeated to test the reversible photoswitching of the PA signal of the nanoprobe. The PA intensities of the sample at the OFF and ON states were calculated to compare the ON/OFF ratio of the nanoprobe.

To test the PA signal of the nanoprobe at different excitation wavelengths, three samples were prepared with the aqueous suspension of the nanoprobe (5 nM, 100 μL) in transparent Eppendorf plastic tubes. The PA images of these samples were first collected in the initial OFF state of the nanoprobe with the excitation at 680, 700, and 750 nm, respectively. Then all the samples were switched ON by scanning with the 980 nm laser, and the PA images were collected again with the excitation at 680, 700, and 750 nm, respectively.

To test the PA signal intensities of the nanoprobe at different concentrations, the aqueous suspension of the nanoprobe was prepared at various concentrations (0.25, 0.5, 1, 2.5, and 5 nM, 100 μL). These samples were switched ON by scanning with the 980 nm laser. Then the PA images of the samples were collected in a transparent Eppendorf plastic tube with the excitation at 680 nm. The PA signal intensities of the nanoprobe at various concentrations in the ON state were calculated to show the relationship between the PA signal amplitude and probe concentration.

Photoacoustic photoswitching imaging (PAPSI). In a typical PAPSI cycle, PA images of the samples were first collected in the initial OFF state of the nanoprobe using a 680 nm pulsed laser (7 ns pulses, 3 mJ, 20 Hz, 1.9 min) for excitation to generate the 'OFF' images. Then the 980 nm laser (scan time 1 min) was applied for switching ON the nanoprobe, and the PA images of the samples were collected again with 680 nm excitation (1.9 min) to generate the 'ON' images. The 680 nm laser also gradually switched OFF the nanoprobe during the PA signal collecting for the next PAPSI cycle. The differential images obtained by subtracting the 'OFF' images from the 'ON' images in each cycle represent just the probe signals. These differential images were then stacked together pixel-by-pixel to generate the "Summed" images.

PAPSI of the nanoprobe in tube phantoms with Hb as the background. The aqueous suspension of the nanoprobe (50 μL) was added to an aqueous solution of human hemoglobin (Hb, 20 mg mL^{-1}, 50 μL, 0.3% oxygen) in a transparent Eppendorf plastic tube to a final concentration of 2.5, 1.25, 0.5, 0.25 or 0.05 nM. Then probe signals were detected by PAPSI, as mentioned above. The PAPSI cycles are 1, 1, 5, 10 and 20 for the probe concentration of 2.5, 1.25, 0.5, 0.25 and 0.05 nM, respectively.

For comparison, the unmixing of the probe signal from the Hb background signal was also tested by subtracting the PA images collected at two different wavelengths.[7,8] The aqueous suspension of the nanoprobe (50 μL) was added to an aqueous solution of human hemoglobin (Hb, 20 mg mL^{-1}, 50 μL, 0.3% oxygen) in a transparent Eppendorf plastic tube to a finial nanoprobe concentration of 2.5, 1.25, and 0.5 nM. The samples were switched ON with the 980 nm laser (3 W, 1 mm bean diameter, scan time 1 min), and PA images were collected with 680 nm excitation. Then the samples were switched ON again, and the PA images were collected with 850 nm excitation. The nanoprobe has a strong absorption at 680 nm while almost no absorption at 850 nm, so the PA images collected at 680 nm contain both probe signals and Hb signals, while PA images collected at 850 nm only contain Hb signals. The probe signals were unmixed from the Hb signals by subtracting the PA images collected at 850 nm from 680 nm.

Cell labeling with the photoswitchable nanoprobe. HeLa cells were cultured in RPMI medium 1640 (GIBCO) containing L-Glutamine, 25 nM HEPES and 10% fetal bovine serum (FBS, GIBCO) under 5% CO_2 and 95% humidified air at 37 °C. For confocal fluorescence microscope imaging, HeLa cells were seeded in 35 mm glass bottom dishes. The nanoprobe suspension in PBS (pH 7.4, 1x) was added to the cell culture medium to a final concentration of 0.125 nM. After incubation for 2, 6, or 10 h at 37 °C,

the cells were washed with PBS (pH 7.4, 1x) three times and imaged on a Zeiss LSM 880 laser scanning confocal microscope. Excitation: 405 nm; Emission: 450 – 550 nm.

To quantify the uptake of the nanoprobe by HeLa cells, HeLa cells were seeded in 6-well cell culture plates and incubated with the nanoprobe at the concentration of 0.125 nM at 37 °C for 2, 6 and 10 h (three wells per group in the 6-well cell culture plates). After incubation, the cells were washed with PBS (pH 7.4, 1x) three times, trypsinized, and collected. The cell numbers were counted using a cell counter. The cell samples were then digested with concentrated nitric acid. The concentrations of Yttrium (Y) in the cell samples were measured using ICP-MS. As the blank reference, the concentration of Y in the cells incubated in the medium only was also measured. The total number of nanoprobes in the samples was calculated using the equation mentioned in the synthesis of the nanoprobe based on Y's concentration. The average number of nanoprobes per cell was obtained by dividing the total number of nanoprobes by the number of cells in the samples. To quantify the uptake of the nanoprobe by HeLa cells at different probe concentrations, HeLa cells were seeded in 6 well cell culture plates and incubated with the nanoprobe at different concentrations (0.0625, 0.125, 0.25, 0.5, 1, and 2 nM, three wells per group in the 6-well cell culture plates) at 37 °C for 6 h. After incubation, the numbers of nanoprobes per cell were determined accordingly.

Cytotoxicity test of the nanoprobe. HeLa cells were seeded in 96-well cell culture plates and incubated with the nanoprobe at different concentrations (0, 0.0625, 0.125, 0.25, 0.5, 1, and 2 nM, six wells per group in the 96-well cell culture plates) in the culture medium at 37 °C for 24 h. MTT (5 mg mL^{-1}, 20 μL) was added to each well, and the cells were incubated for 3 h at 37 °C. Then the cell culture medium was replaced with DMSO (200 μL for each well). The 96 well cell culture plates were gently shaken for 10

min at room temperature to dissolve the formed compound. The absorbance of each well at 570 nm was recorded on a microplate reader (Tecan Safire). Cell viability was calculated by the ratio of the absorbance of the cells incubated with the nanoprobe to cells incubated with culture medium only.

PAPSI of the nanoprobe in the cells. HeLa cells were incubated with the nanoprobe (1 nM) at 37 °C for 6 h, followed by three washes with PBS (pH 7.4, 1x). After trypsinization, the cells were collected and counted using a cell counter. Then these cells were transferred in a transparent Eppendorf plastic tube in 10 μL PBS for PAPSI. For cell number of 10^6 and 10^5, only one cycle of PAPSI was performed. For the cell number of 2×10^4 and 5×10^3, 5 and 20 cycles of PAPSI were performed, respectively.

Animal experiments. All animal experiments were performed in compliance with the Guidelines for the Care and Use of Research Animals established by the Stanford University Institutional Animal Care and Use Committee. NU/NU nude mice (5 – 6 weeks, female, Charles River Laboratories International, Inc.) were used in all animal experiments. Mice were randomly distributed to different groups. The investigators were not blind to the treatment information of the groups before data analysis.

Safety of the laser exposure on the skin of the mice. A small skin region (diameter around 1 cm) on the back of the NU/NU nude mice was selected and repeatedly exposed to the 980 nm laser 20 times. Each time the selected skin region was scanned with the laser beam for 1 min. The time interval was 1 min between each exposure. After each exposure, the skin was checked to see whether there was any burn injury, and the photographs of the skin were recorded.

To study the thermal effect of the 980 nm laser and the kinetics of the following cooling procedure, the heat maps of the nude mouse were captured by a thermal camera before, 0, 3, 6, 9, 12, 15 and 54 s after laser exposure. The real-time temperature of the laser-irradiated region on the mouse's back was measured at each time point.

When applying PAPSI for mouse imaging, the 980 nm laser beam was scanned over the targeted area (diameter around 1 cm) on the mouse skin for 1 min in each PAPSI cycle (4.8 min for each cycle).

Cell tracking with the photoswitchable nanoprobe in the living mice. After incubated with the nanoprobe (1 nM) at 37 °C for 6 h, HeLa cells (10^6, 10^5 and 10^4) in 10 μL PBS (containing 50% Corning Matrigel) were subcutaneously implanted to the back of the NU/NU nude mice (three mice per group) for PAPSI. Before PA imaging, the positions of the mice were manually adjusted in the bright field to make the cell-implanted spot at a fixed coordinate in the field of view to predetermine the location of the cells in the obtained PA images. 5, 10, and 20 cycles of PAPSI were performed for the cell number of 10^6, 10^5, and 10^4, respectively.

Imaging depth of PAPSI with the nanoprobe. A PE tube filled with the aqueous suspension of the nanoprobe (5 nM) was inserted with a 45° angle to a cubic pork ham phantom with a thickness of 2 cm (absorption coefficient μ_a ~ 0.12 cm^{-1}, reduced scattering coefficient μ_s ~ 3.6 cm^{-1}).[9] To avoid the potential disturbance of the air, the end of the PE tube stopped at about 0.2 cm from the bottom of the cubic phantom. The phantom was placed in the Endra Nexus 128 *in vivo* PA imaging system, and the PA images were first collected in the initial OFF state of the nanoprobe at 680 nm. Then the phantom was raster scanned with the 980 nm laser (scan time 2 min) from the

bottom of the phantom to switch ON the nanoprobe, followed by PA imaging again at 680 nm. The PA images were reconstructed, and the PA signals from the PE tube in the XZ cross-section were obtained to show the imaging depth.

PA image processing and analysis. The original data of PA imaging were reconstructed with the commercial software of the Endra Nexus 128 *in vivo* PA imaging system. The data were exported as DICOM files and read into OsiriX (v 9.0, Pixmeo SARL). For cycled PAPSI, the top views of the PA images were obtained and exported as gray images in TIFF format. The gray images were imported into Matlab (v 9.0.0, MathWorks), where the OFF images were subtracted from the ON images, and the differential images were added together to generate the accumulated probe signals. Negative pixel values were allowed in the obtained differential images, which helped reduce the background noise in the stacked images due to the random distribution of the background signals.

Statistical analysis. Statistical analysis was performed using GraphPad Prism (v 7.0, GraphPad Software, Inc.). Comparisons between two groups were determined by t-test. * $p < 0.05$, ** $p < 0.01$. A p value of < 0.05 was considered to be statistically significant. The results are presented as Mean ± SD unless otherwise stated.

Toxicity study. NU/NU nude mice were either injected with nanoprobe (20 nM, 100 μL) or saline *via* tail vein. Mice were observed daily to monitor if they remained healthy for 1 week. The liver, spleen, kidneys, lungs, and heart were harvested 1 week after I.V injection of nanoprobe. Tissues were immediately transferred to formalin bath and were further processed for H & E staining.

Supporting Figures

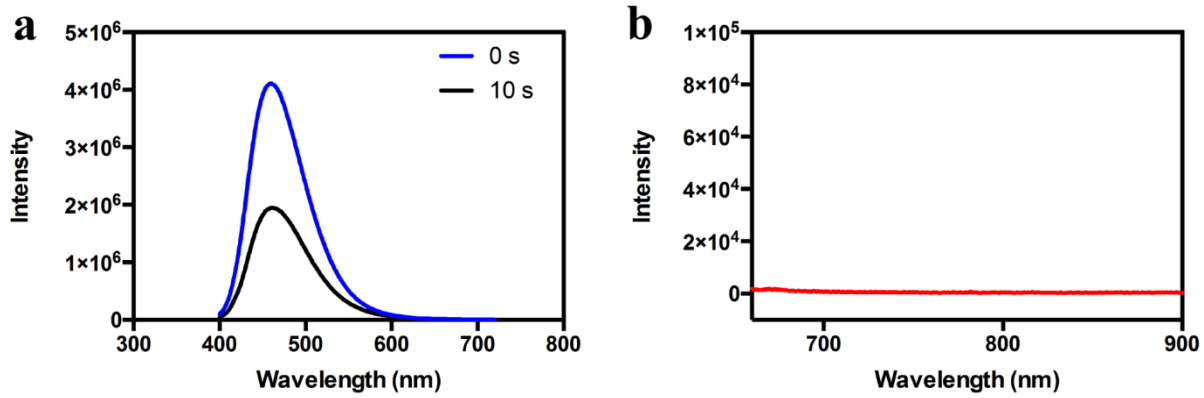

Figure S1. The photoluminescence properties of the photoswitchable small molecule. (a) Emission spectra of the photoswitchable small molecule in $CHCl_3$ (5 μg mL^{-1}) in the initial open state (0 s) and after switched to the closed state by exposure to the 365 nm UV lamp for 10 s. Excitation: 370 nm. (b) The emission spectrum of the closed form of the photoswitchable small molecule in $CHCl_3$ (5 μg mL^{-1}) upon the excitation at 640 nm.

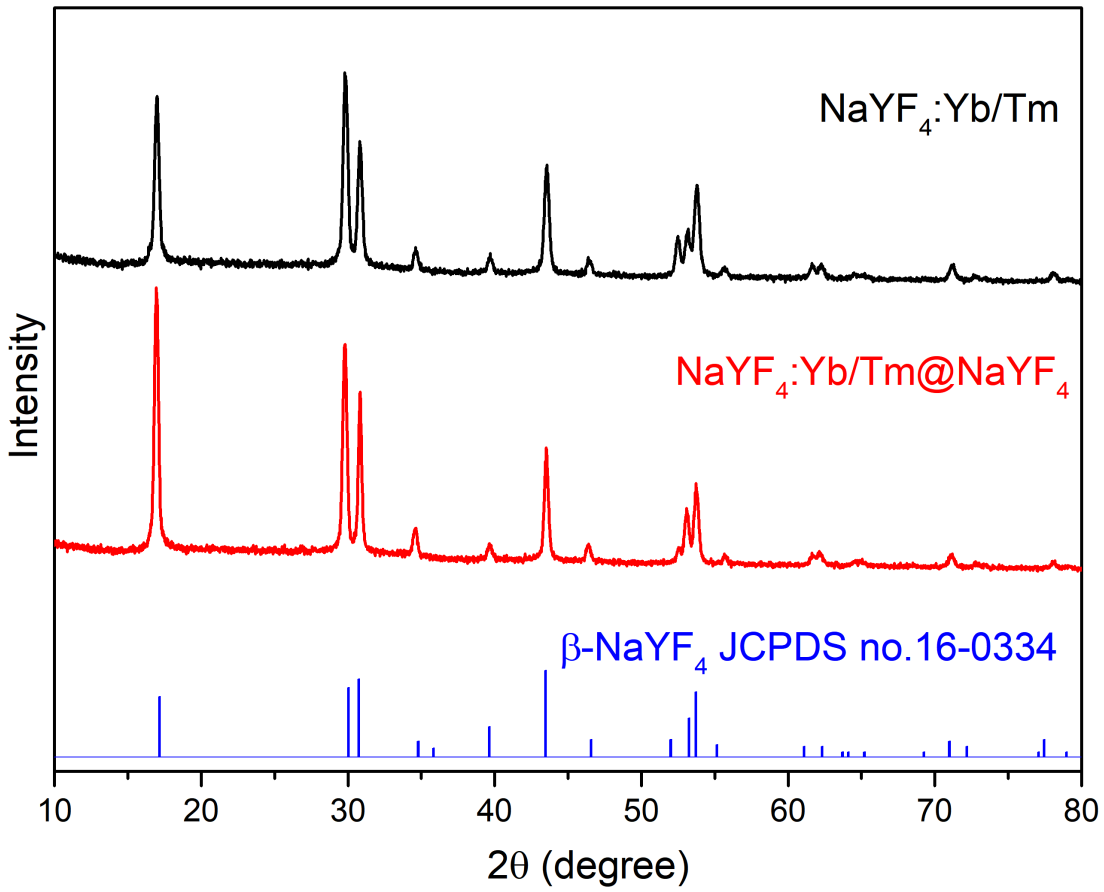

Figure S2. The X-ray diffraction (XRD) patterns of the core/shell UCNP. The corresponding XRD patterns of $NaYF_4$:Yb/Tm and $NaYF_4$:Yb/Tm@$NaYF_4$ nanoparticles showed peak positions that can be well indexed as hexagonal $NaYF_4$ (JCPDS file number 16-0334), demonstrating the high-quality of the samples.

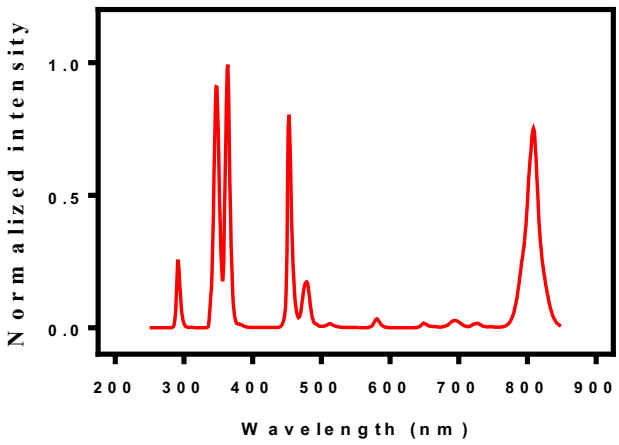

Figure S3. Emission spectrum of the core/shell UCNP in $CHCl_3$ (0.5 mg mL^{-1}) under the excitation of 980 nm laser (1 W, laser beam diameter = 1 mm).

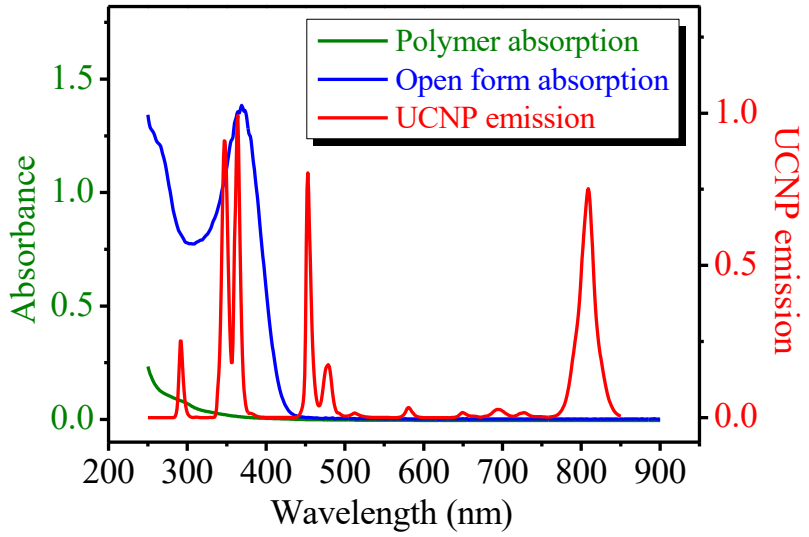

Figure S4. Overlap between the emission spectrum of the UCNP and the absorption spectra of 3ThacacH (in the open form, 0.5 mg mL^{-1}) and amphiphilic polymer (5 mg mL^{-1}). Note that the amphiphilic polymer has nearly no absorption at the two major UV emission peaks of UCNP (345 and 362 nm) and a weak absorption at the small 290 nm emission peak of the UCNP. The absorbance of the amphiphilic polymer at 290 nm is 100-fold lower than that of 3ThacacH (in the open form) at the same mass concentration.

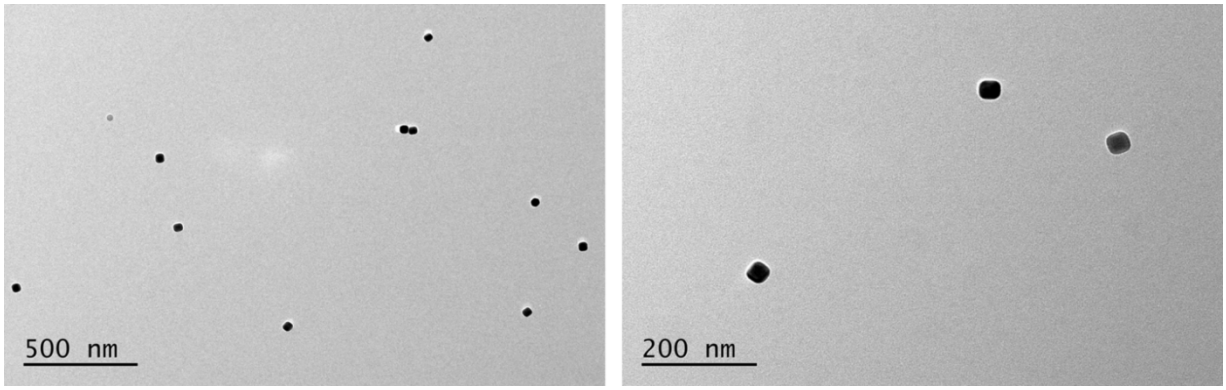

Figure S5. TEM images of the photoswitchable PA nanoprobe.

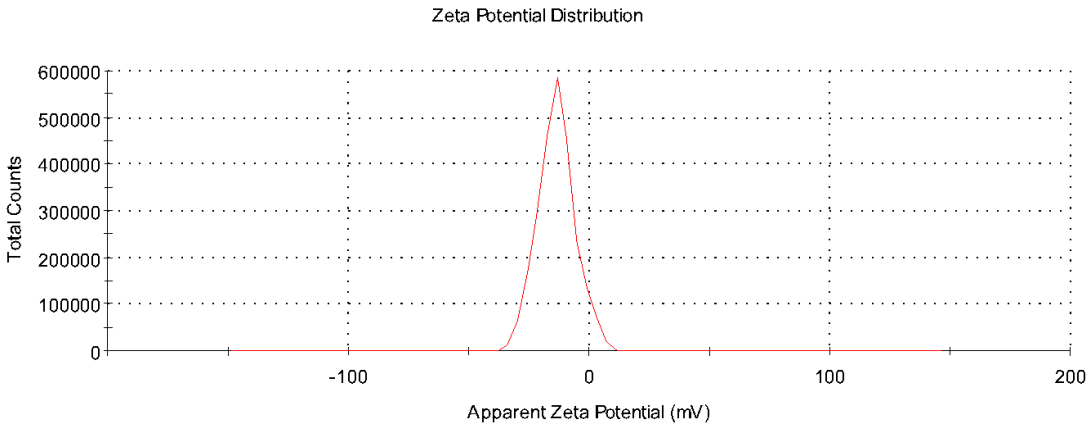

Figure S6. Zeta potential distribution of the nanoprobe measured on a Zetasizer Nano ZS90 dynamic light scattering (DLS) analyzer (Malvern Instruments). Mean zeta potential: -13.6 mV; Zeta Deviation: 7.64 mV.

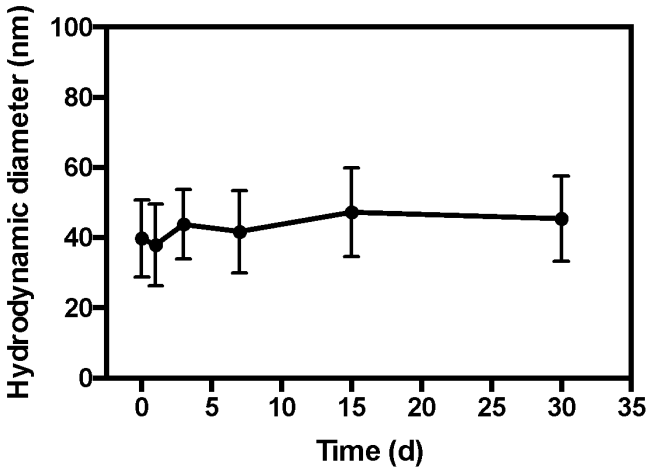

Figure S7. Stability test of the PAPSI probe. Freshly prepared nanoprobes in PBS buffer (pH 7.4, 1x) were stored at 4 ºC. The hydrodynamic diameter of the sample was measured at 0, 1, 3, 7, 15, and 30 d. The result shows that the size of the nanoprobe did not increase significantly within 30 days (varying in the range of 40 to 50 nm). The results are Mean ± SD from 10 DLS measurements.

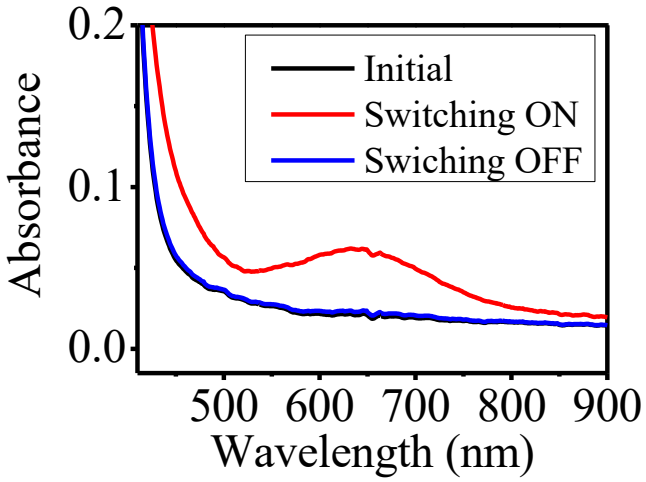

Figure S8. Absorption spectra of the nanoprobe in water (2.5 nM) when switched ON with 980 nm laser (average power density 3 W/cm^2 for 1 min scan) and switched OFF with 640 nm laser (average power density 10 mW/cm^2, 10 s).

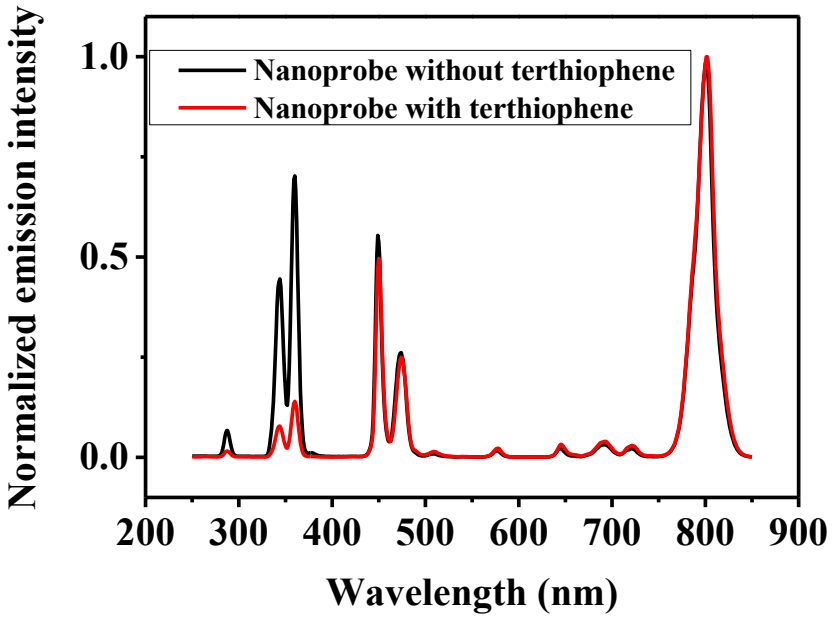

Figure S9. Comparison of the emission spectra of the nanoprobes (2.5 nM) with or without 3ThacacH in distilled water with the excitation at 980 nm. The encapsulation of 3ThacacH caused a significant decrease in the emission intensity of the UCNP in the UV range (250–400 nm) but not in the NIR range (750–850 nm). The emission intensity of the UCNP reduced by 82.8% at 345 nm and 80.2% at 362 nm. Note that the amphiphilic polymer existed in both nanoprobes, so the decrease of the UV emission should have just come from the absorption of and transfer to the 3ThacacH molecule. The quantum yield of the UV emission (250 – 400 nm) of the UCNP encapsulated in the amphiphilic polymer in water was determined to be 0.0412%, which is 31.2% of that in $CHCl_3$.

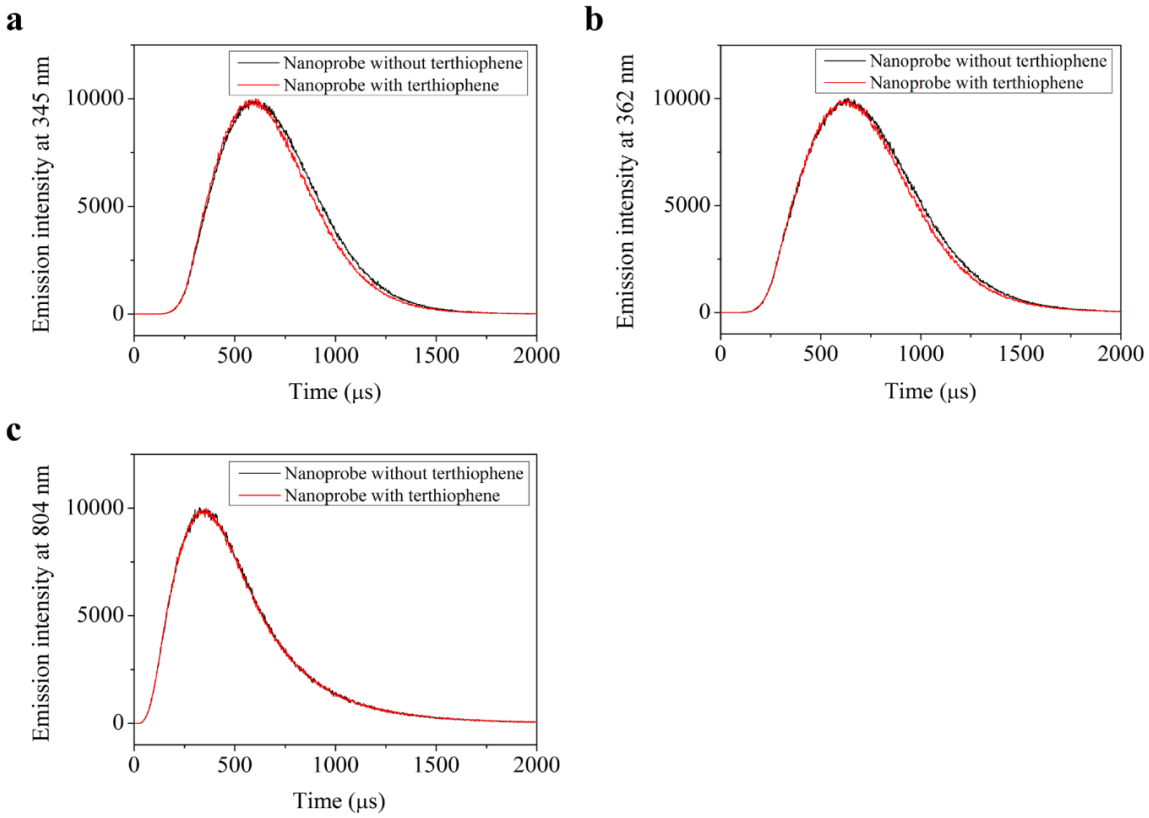

Figure S10. Comparison of the lifetime of the nanoprobes with or without encapsulated 3ThacacH in distilled water at various emission wavelengths (345, 362, and 804 nm) with the excitation at 980 nm. The addition of 3ThacacH caused a small decrease of the lifetime of the UCNP in the UV range (from 0.336 to 0.308 μs at 345 nm and from 0.408 to 0.378 μs at 362 nm), but little change of the lifetime in the NIR range (804 nm). The resonance energy transfer efficiency (ET) can be calculated with the formula: $ET = 1 - \frac{\tau_{DA}}{\tau_D}$, where τ_{DA} and τ_D are the lifetimes of the donor with and without acceptor, respectively. The resonance energy transfer efficiency from the UCNP to 3ThacacH was calculated to be 8.33% at 345 nm and 7.35% at 362 nm.

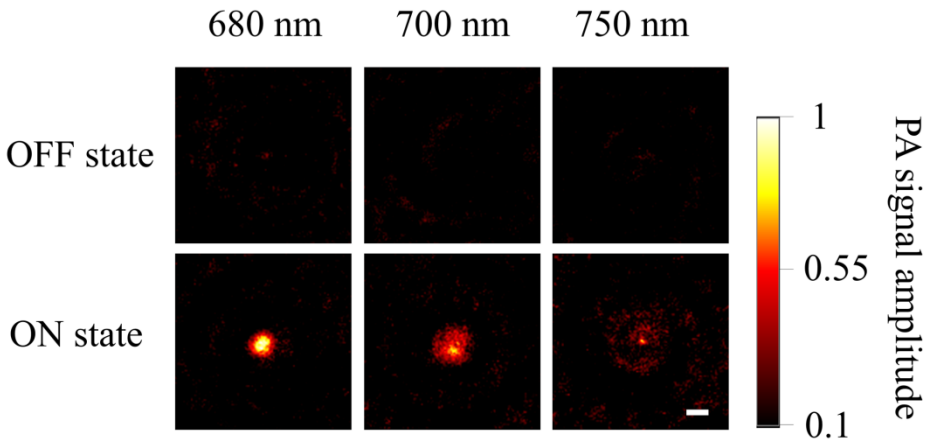

Figure S11. The PA signals of the nanoprobe at different excitation wavelengths. The aqueous suspension of the nanoprobe (5 nM, 100 μL) in a transparent plastic tube was imaged in the Endra Nexus 128 *in vivo* PA imaging system at 680, 700, 750 nm before and after being switched ON with 980 nm light. Scale bar: 2 mm.

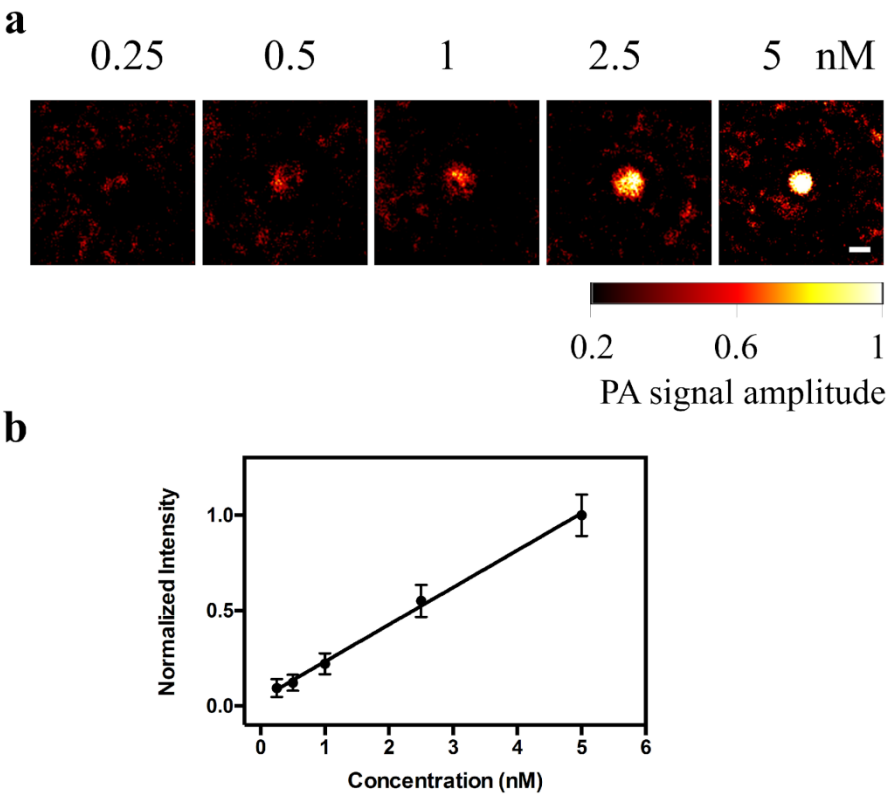

Figure S12. The PA signals of the nanoprobe at different concentrations in the ON states. (a) The PA images of the aqueous suspension of the nanoprobe at various concentrations (0.25 to 5 nM, 100 μL) in a transparent plastic tube were collected in the Endra Nexus 128 *in vivo* PA imaging system with 680 nm excitation after switched ON with 980 nm light. Scale bar: 2 mm. (b) The linear relationship between the PA signal amplitude of the nanoprobe in the ON state and the probe concentration.

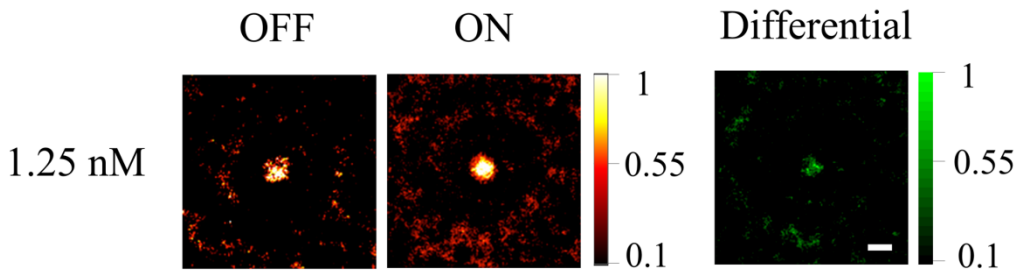

Figure S13. PAPSI of the nanoprobe (50 μL) mixed with hemoglobin (Hb) solution (20 mg mL^{-1}, 50 μL) in a transparent plastic tube to a final probe concentration of 1.25 nM. The differential image is obtained by subtracting the OFF image from the ON image. Scale bar: 2 mm.

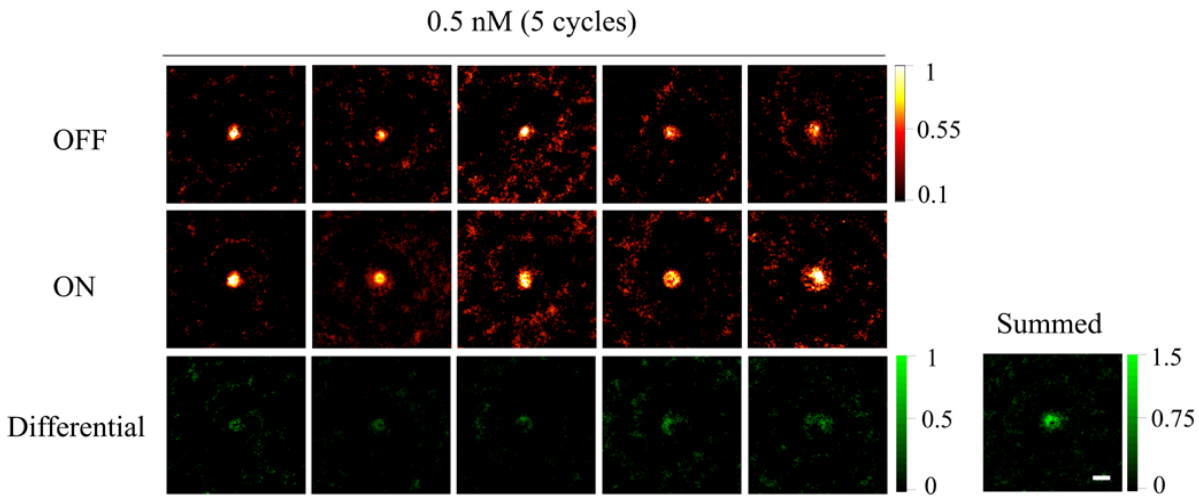

Figure S14. Detecting the nanoprobe (50 μL) mixed with Hb solution (20 mg mL^{-1}, 50 μL) in a transparent plastic tube to a final probe concentration of 0.5 nM by 5 cycles of PAPSI. The differential images obtained in the PAPSI cycles were stacked pixel-by-pixel to generate the "Summed" image (this protocol applies to all summed images). Scale bar: 2 mm.

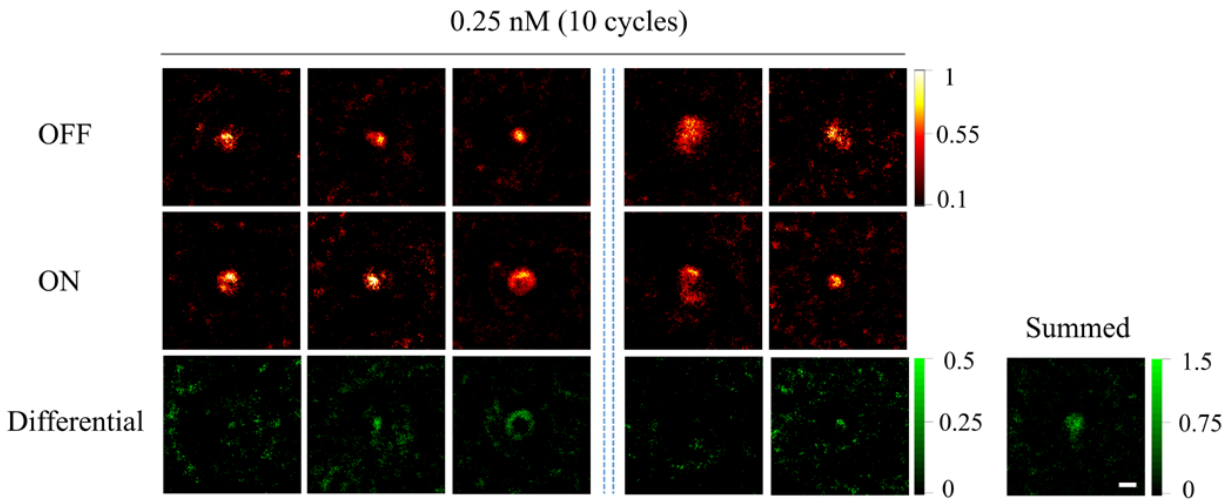

Figure S15. Detecting the nanoprobe (50 μL) mixed with Hb solution (20 mg mL^{-1}, 50 μL) in a transparent plastic tube to a final probe concentration of 0.25 nM by 10 cycles of PAPSI. The PA images collected in the first 3 and last 2 cycles are shown. The summed image was generated as before. Scale bar: 2 mm.

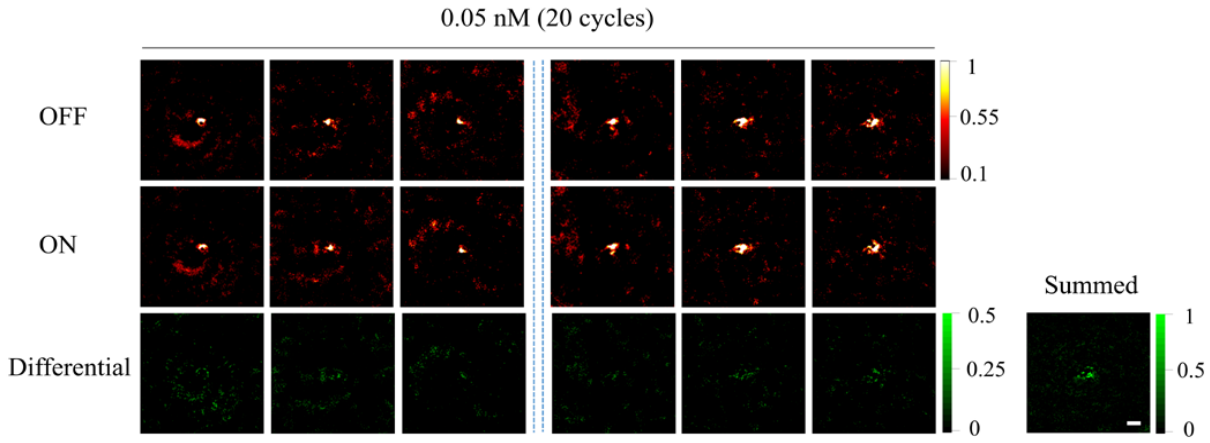

Figure S16. Detecting the nanoprobe (50 μL) mixed with Hb solution (20 mg mL^{-1}, 50 μL) in a transparent plastic tube to a final probe concentration of 0.05 nM by 20 cycles of PAPSI. The PA images collected in the first 3 and last 3 cycles are shown. The summed image was generated as before. Scale bar: 2 mm.

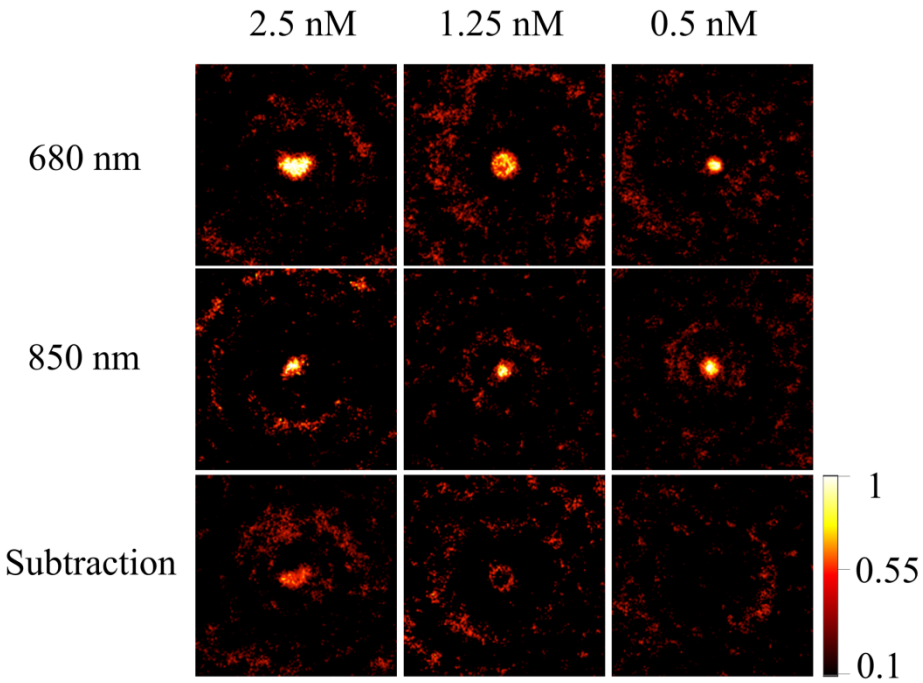

Figure S17. Detecting the probe signal from the nanoprobe/Hb mixture by subtracting PA images at two different wavelengths. The aqueous suspension of the nanoprobe (50 μL) was added to the hemoglobin (Hb) solution (20 mg mL^{-1}, 50 μL) in a transparent plastic tube to the final probe concentration of 2.5, 1.25, or 0.5 nM. The nanoprobe was switched ON by a 980 nm laser, and the PA images of these samples were collected with 680 nm excitation. Then the samples were switched ON again, and the PA images were collected with 850 nm excitation. The PA images that only represent the signal of the nanoprobe were obtained by subtracting the PA images at valley wavelength (850 nm) from the PA images at the peak wavelength (680 nm) according to the absorption spectrum of the nanoprobe.

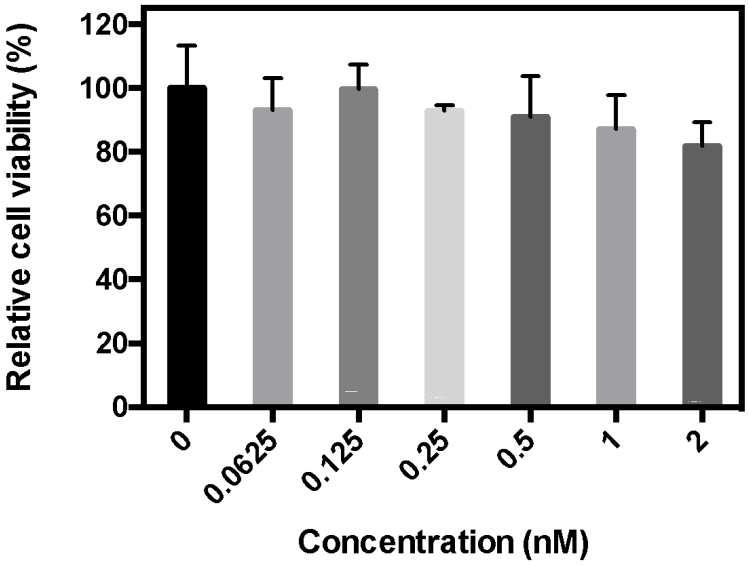

Figure S18. Cytotoxicity of the nanoprobe. HeLa cells were incubated with the nanoprobe at 0 to 2 nM in the culture medium at 37 ºC for 24 h. The cell viability was measured using the MTT assay. Results are presented as Mean ± SD (six wells per group in 96-well culture plates).

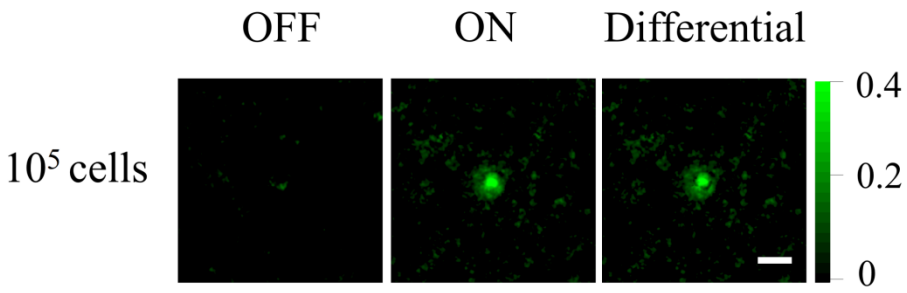

Figure S19. Images of 10^5 labeled cells (2×10^4 NPs per cell) in a transparent plastic tube by one PAPSI cycle. Scale bar: 2 mm.

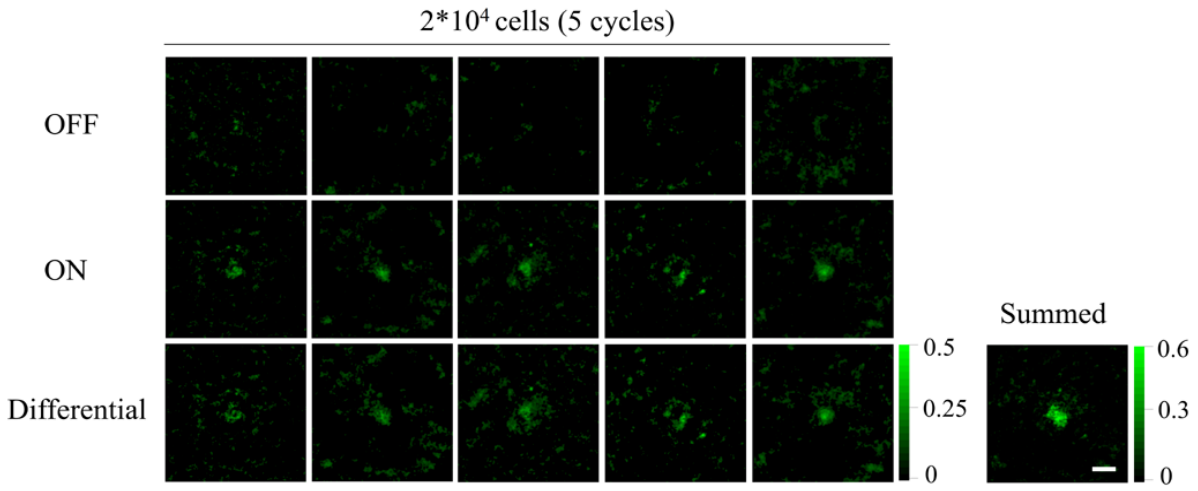

Figure S20. Images of 2 × 10^4 labeled cells in a transparent plastic tube by 5 cycles of PAPSI. The summed image was generated as before. Scale bar: 2 mm.

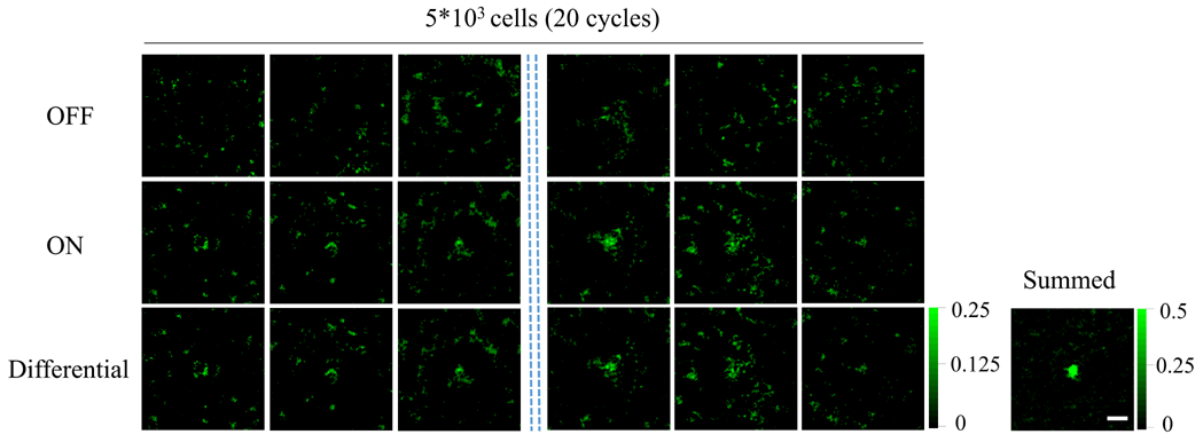

Figure S21. Imaging of 5 × 10^3 labeled cells in a transparent plastic tube by 20 cycles of PAPSI. The PA images of the first and last 3 cycles are presented. The summed image was generated as before. Scale bar: 2 mm.

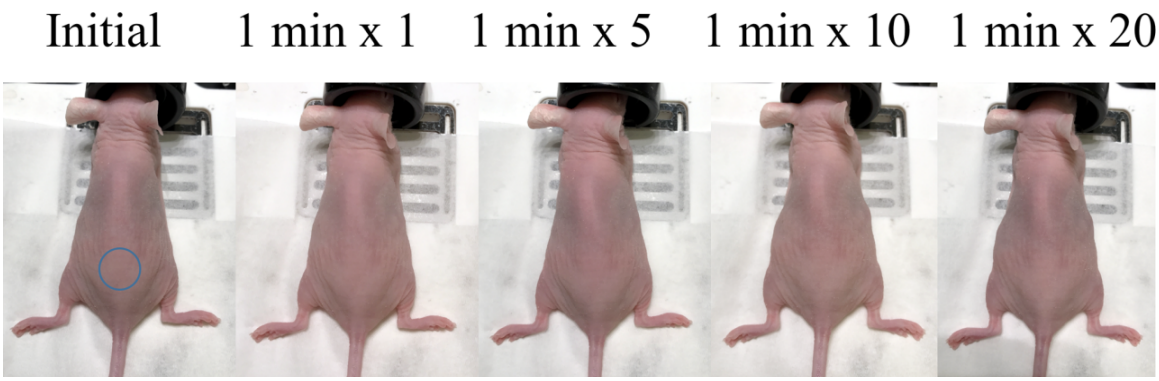

Figure S22. The effect of the switching ON laser 980 nm on the skin of the NU/NU nude mice. The mouse skin was repeatedly exposed to the 980 nm laser (up to 20 times), and each exposure lasted for 1 min with an interval of 1 min in between. The blue circle indicates the region exposed to the laser irradiation and where the HeLa cells loaded with the nanoprobe would be injected.

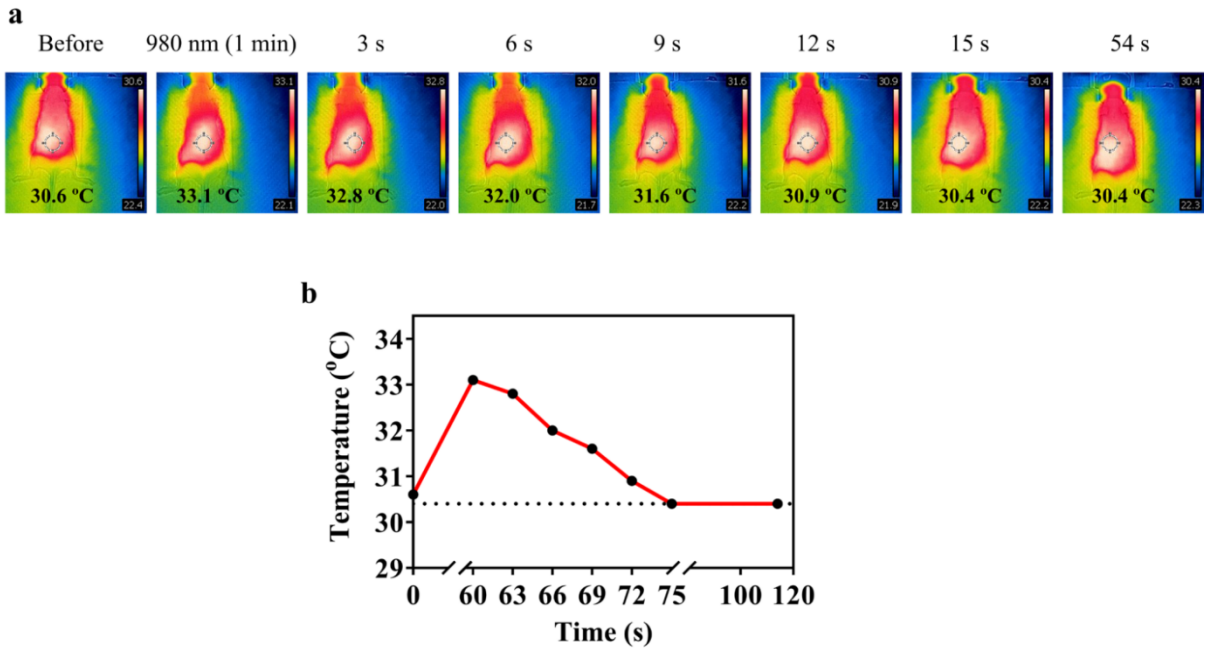

Figure S23. Heating effect of the 980 nm switching ON laser and the cooling kinetics. (a) The selected region (diameter ~ 1 cm) on the back of a NU/NU nude mouse (as indicated in Figure S22) was exposed to the 980 nm laser for 1 min. The heat maps of the mouse were captured by a thermal camera before, 0, 3, 6, 9, 12, 15, and 54 s after exposure. The real-time temperature of the laser-irradiated region was measured at each time point. (b) The plot of the peak temperature of the laser-irradiated region over time. At each time point, the peak heating value is presented. The temperature recovered to its original value in 15 s after laser irradiation, which is much shorter than the time interval of 54 s between the switching ON step and the following PA signal acquisition step in each PAPSI cycle (the total 1.9 min PA imaging time contains 0.9 min for system preparation and 1 min for PA signal acquisition). Therefore, the heating effect induced by the switching ON laser will not cause a temperature difference in the OFF and ON imaging in each PAPSI cycle.

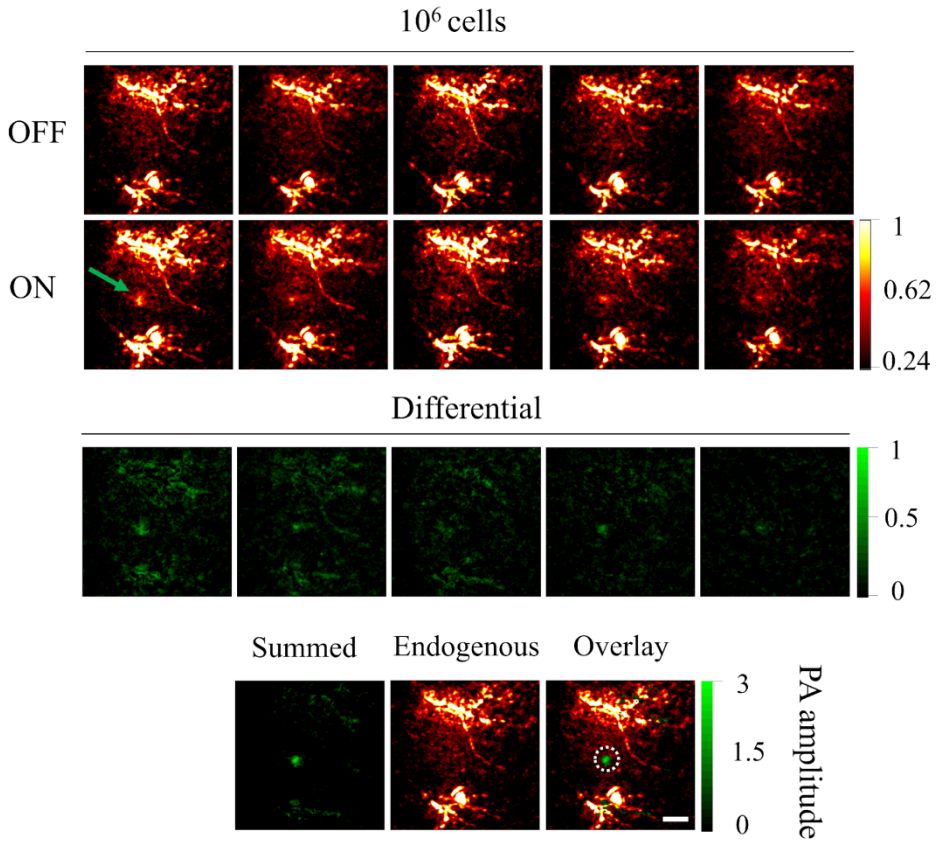

Figure S24. Imaging 10^6 labeled HeLa cells on the back of the mice by 5 cycles of PAPSI. Scale bar: 2 mm. The summed image of the differential images in all PAPSI cycles is demonstrated and overlaid with the endogenous PA signals (the OFF image of the first PAPSI cycle). The white circle indicates the location of the injected cells.

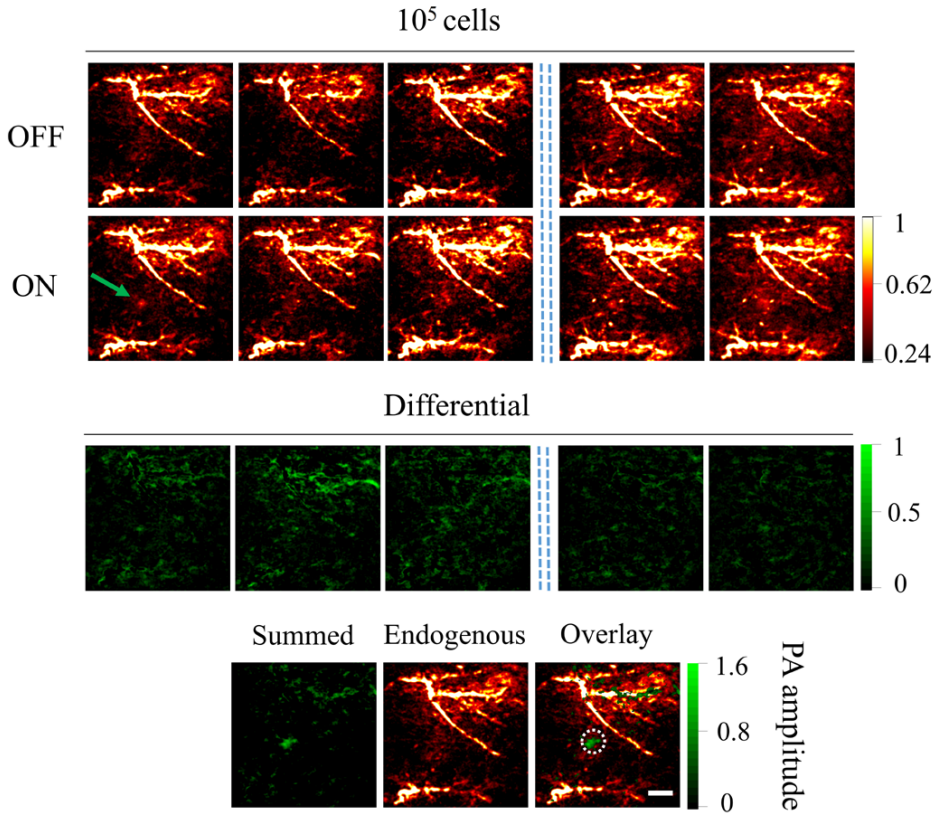

Figure S25. Imaging 10^5 labeled HeLa cells on the back of the mice by 10 cycles of PAPSI. PA images of the first 3 and last 2 cycles are presented. The images were processed using the same method as in Figure S23. Scale bar: 2 mm.

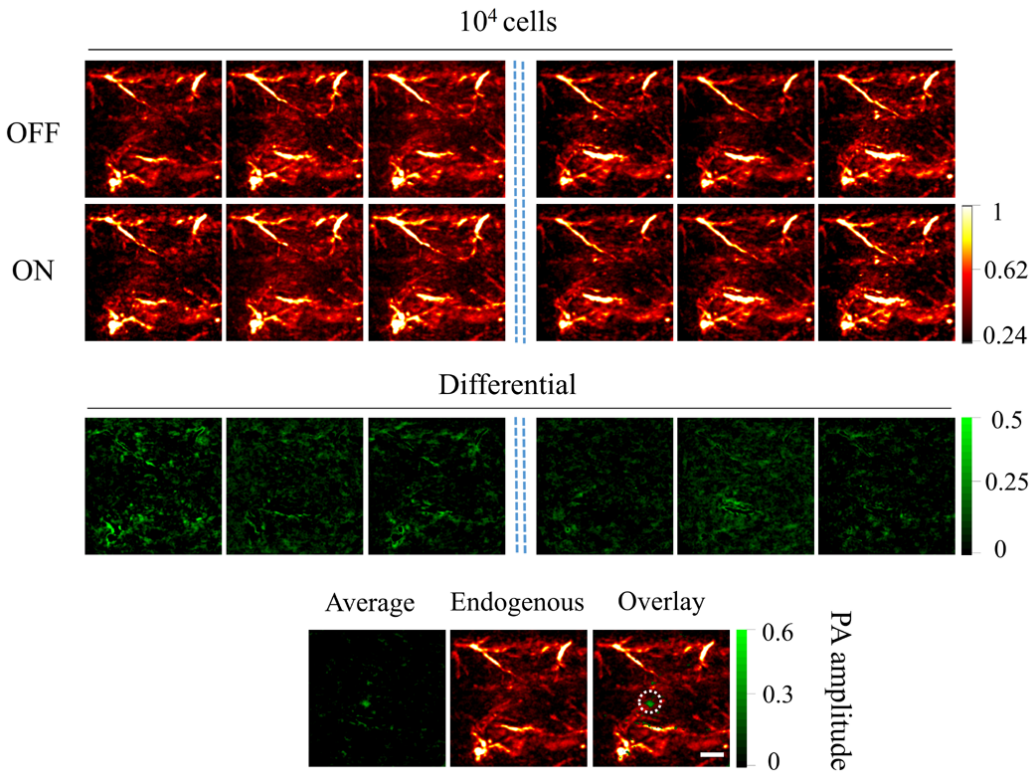

Figure S26. Imaging 10^4 labeled HeLa cells on the back of the mice by 22 cycles of PAPSI. The images were processed using the same method as in Figure S23. The white dashed circle indicates the pre-determined position of the injected cells, which has the sample coordinate in the field of view with that of 10^6 or 10^5 cells (Figure S23 and S24). PA images of the PAPSI cycle 1-3 and 18-20 are presented. Scale bar: 2 mm.

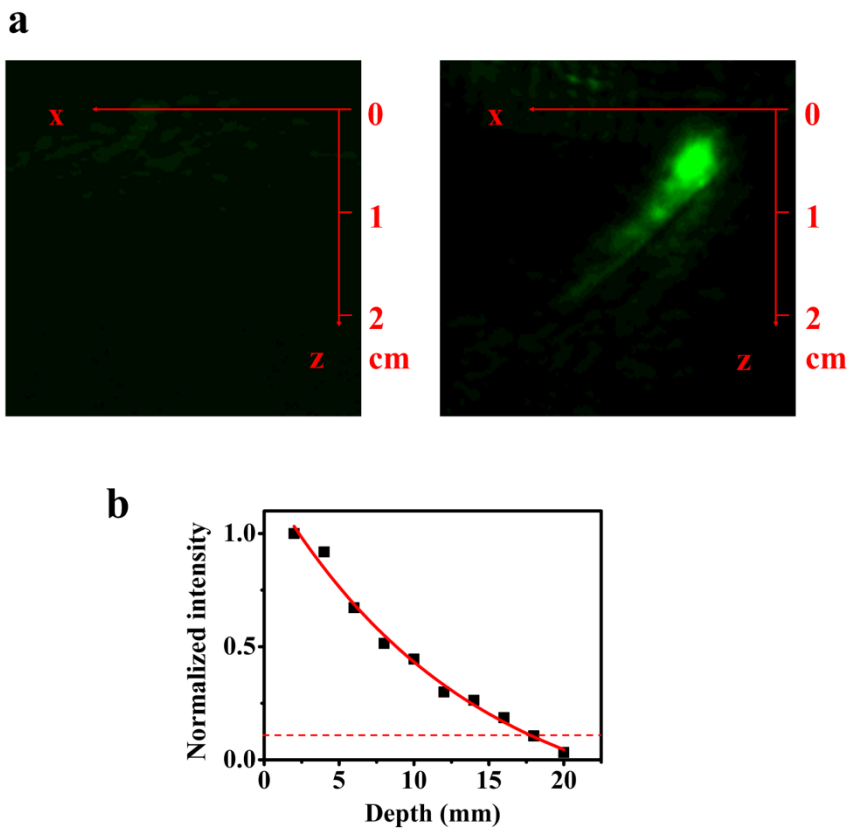

Figure S27. Imaging depth of PAPSI. A PE tube filled with the aqueous suspension of the nanoprobe (5 nM) was inserted at a 45° angle into a cubic pork ham phantom with a thickness of 2 cm. The end of the PE tube stopped at about 0.2 cm from the bottom of the phantom. The PA images of the phantom were first collected in the initial OFF state of the nanoprobe with the excitation at 680 nm. Then the phantom was switched ON from the bottom with a 980 nm laser (average power density of 3 W/cm^2, 2 min scan), and the PA images in the ON state were collected again with 680 nm excitation. The PA images of the PE tube in the XZ cross-section show the imaging depth. (a) Left: PA image of the PE tube in the OFF state. Right: PA image of the PE tube in the ON state (One PAPSI cycle). (b) The PA signal intensities (per unit area) are plotted versus the depth of the phantom tube. The red dash line indicates the threshold for detectable PAPSI signal (10% of maximum intensity), corresponding to a depth of about 1.8 cm.

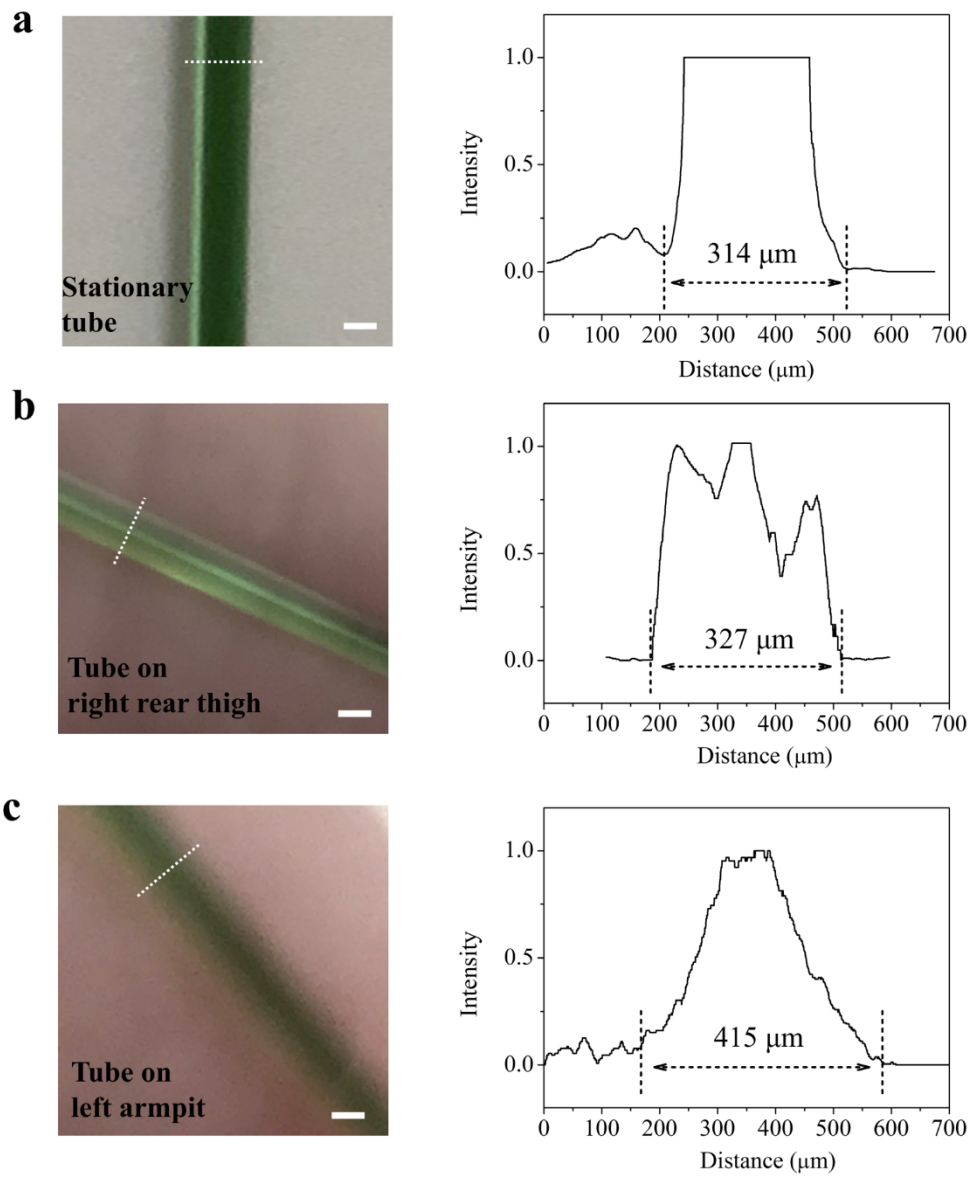

Figure S28. Evaluating the effect of respiration motion on the determination of the diameter of an artificial blood vessel. A NU/NU nude mouse was anesthetized with 1.5% isoflurane and fixed on the holder. A thin capillary tube (diameter ~314 μm, length ~2 cm, filled with a concentrated ICG solution for clear visualization) adhered to the mouse's right rear thigh or left armpit. The bright-field images of the tube were captured with a frame rate of 2 fps over 1 min. All images were stacked to obtain the averaged images, which should be subject to the respiration motion. The averaged images of the tube (a) in the stationary state, (b) on the right rear thigh of the mouse, (c) on the left armpit of the mouse are demonstrated and compared. The line profiles on the right

side show the diameter of the tube measured in the corresponding images. Scale bar: 200 μm. Note that the respiration motion tends to have a minor influence on the right rear thigh of the mouse but a larger influence on the left armpit, which is much closer to the diaphragm.[10]

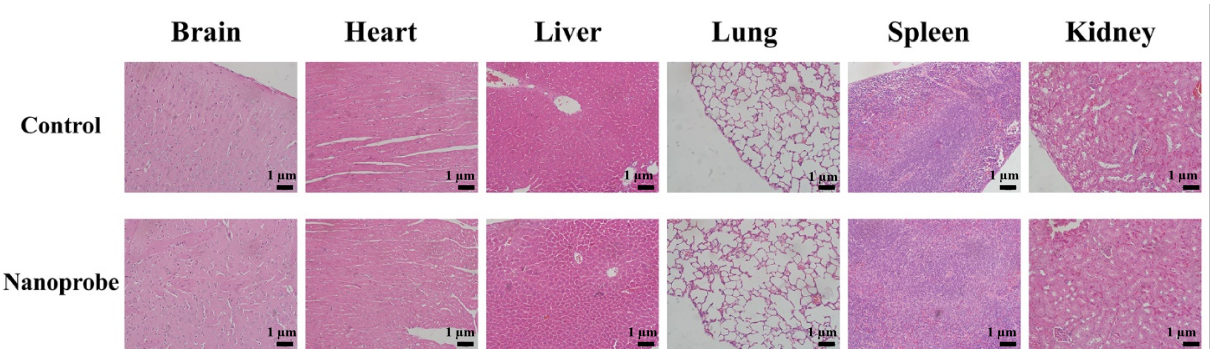

Figure S29. H & E staining of mouse organs harvested 1 week after I.V injection of nanoprobe (20 nM, 100 μL).

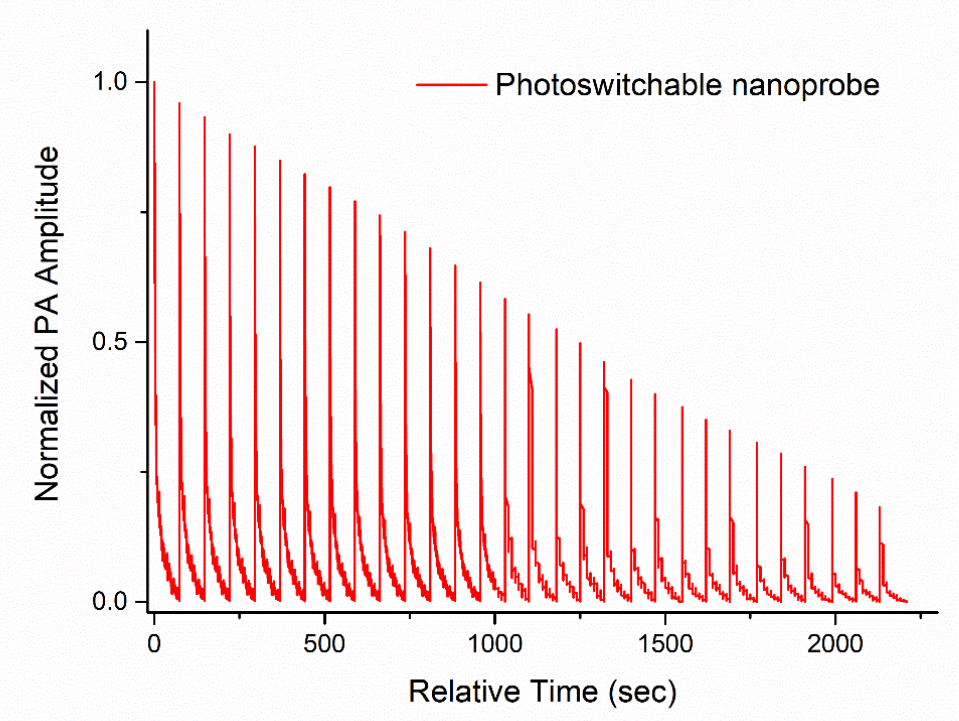

Figure S30. Kinetics of PA signal of photoswitchable nanoprobes upon multiple switching cycles with 980 nm and 680 nm lasers. Shown are 30 switching cycles of the photoswitchable nanoparticles (5 nM), and the PA signal acquisition was performed by a Vevo 3100 LAZR-X system (FULIFILM VisualSonics Inc.). Photoswitching OFF laser pulse is the same as the PA imaging laser, 680 nm (pulse rate 20 Hz, laser power on sample 3-6 mJ per pulse, pulse width < 10 ns, transducer frequency 15 MHz, frame rate 5 fps, record time ~ 70 s per cycle). Photoswitching ON by the CW980 laser (average power density 3 W/cm^2, irradiation time: 60 s). The kinetics of the photoswitching OFF process per cycle was recorded in real time by measuring the PA signal changes during PA imaging acquisition. The photoswitching ON process per cycle was not recorded because the PA excitation laser was OFF while the CW980 laser was ON.

Supporting Tables

Concentration (nM)	2.5	1.25	0.5		0.25		0.05	
Cycles	1	1	1	5	1	10	1	20
CNR	22.89 ± 5.65	12.52 ± 4.64	6.46 ± 1.44	16.80 ± 2.63	0.85 ± 0.15	8.53 ± 2.50	0.163 ± 0.013	3.89 ± 0.88

Table S1. The contrast-to-noise ratio (CNR) of the PA signals from the nanoprobe (50 μL) mixed with Hb solution (20 mg mL^{-1}, 50 μL) to various final concentrations and imaged with PAPSI. CNR = $\frac{I_{ROI}-I_B}{\sigma_B}$ where I_{ROI} is the mean pixel intensity of the ROI, I_B is the mean intensity of the positive pixels in the background, and σ_B is the standard deviation of the pixel intensities in the background. Results are presented as Mean ± SD. In each PA image (field of view 12×12 mm), the PA signal amplitude of the nanoprobe sample was measured in an ROI (with the size of 1.5×1.5 mm) in the center of the sample location, and the noise signal was measured in another three ROIs (with the size of 3×3 mm) randomly selected near the periphery of the field of view. The calculation method of CNR was used for all the phantom studies. The CNR of 3.89±0.88 in the detection of 0.05 nM nanoprobe in the Hb solution by 20 PAPSI cycles corresponds to a confidence interval of 1.71 to 6.07 at a confidence level of 95%.

Strategy	$Image_{680} - Image_{850}$		
Concentration (nM)	2.5	1.25	0.5
CNR	7.38 ± 1.75	1.56 ± 0.53	Not detectable

Table S2. The nanoprobe (50 μL) was mixed with Hb solution (20 mg mL^{-1}, 50 μL) to various final concentrations (0.5 to 2.5 nM). The PA signals of the nanoprobe were obtained by subtracting the PA images at 850 nm from the PA images at 680 nm. Results are presented as Mean ± SD (calculated with the same method as for Table S1).

Cell number	10^6	10^5	$2*10^4$		$5*10^3$	
Cycles	1	1	1	5	1	20
CNR	20.86 ± 4.18	4.08 ± 1.01	1.52 ± 0.38	7.64 ± 1.98	-0.448 ± 0.104	8.94 ± 1.65

Table S3. The CNR of the HeLa cells labeled with the nanoprobe (2×10^4 NPs per cell) and imaged in the tube phantoms at varying cell numbers (10^6 to 5×10^3) and different photoswitching cycles (1 to 20). Results are presented as Mean ± SD (calculated with the same method as for Table S1).

Cell number	10^6		10^5		10^4	
Cycles	1	5	1	10	1	22
CNR	1.79 ± 0.38	7.50 ± 1.64	0.240 ± 0.036	2.78 ± 0.45	0.0292 ± 0.0052	2.44 ± 0.56

Table S4. The CNR of the HeLa cells loaded with the nanoprobe (2×10^4 NPs per cell) and imaged in the back of the living mice at indicated cell numbers and photoswitching cycles. Results are presented as Mean ± SD (calculated with the same method as for Table S1, except that the ROI size for the probe signal was 1×1 mm).

Items	Results
Mass of UCNP (mg)	0.5
Effective diameter of UCNP particle (nm)	35
Volume of single UCNP particle (cm^3)	2.2×10^{-17}
Density of $NaYF_4$ (g/cm^3)	4.23
Molar mass of UCNP (g/mol)	5.7×10^{7}
Quantity of UCNPs (mol)	8.7×10^{-12}
Mass of 3ThacacH (mg)	0.05
MW of 3ThacacH (g/mol)	389
Quantity of 3ThacacH (mol)	1.2×10^{-7}
3ThacacH : UCNP	1.4×10^{4}

Table S5. Estimation of the approximate number of 3ThacacH in each photoswitchable nanoprobe.

References

[1] X. Chen, L. Jin, W. Kong, T. Sun, W. Zhang, X. Liu, J. Fan, S. F. Yu, F. Wang, *Nat. Commun.* **2016**, *7*, 10304.

[2] R. A. Kruger, R. B. Lam, D. R. Reinecke, S. P. Del Rio, R. P. Doyle, *Med. Phys.* **2010**, *37*, 6096–6100.

[3] D. Van de Sompel, L. S. Sasportas, J. V. Jokerst, S. S. Gambhir, *PLoS One* **2016**, *11*, e0152597.

[4] S. E. Bohndiek, S. Bodapati, D. Van De Sompel, S.-R. Kothapalli, S. S. Gambhir, *PLoS One* **2013**, *8*, e75533.

[5] C.-T. Poon, W. H. Lam, V. W.-W. Yam, *Chem. - A Eur. J.* **2013**, *19*, 3467–3476.

[6] A. E. Albers, E. M. Chan, P. M. McBride, C. M. Ajo-Franklin, B. E. Cohen, B. A. Helms, *J. Am. Chem. Soc.* **2012**, *134*, 9565–9568.

[7] E. Huynh, B. Y. C. Leung, B. L. Helfield, M. Shakiba, J.-A. Gandier, C. S. Jin, E. R. Master, B. C. Wilson, D. E. Goertz, G. Zheng, *Nat. Nanotechnol.* **2015**, *10*, 325–332.

[8] J. R. Casar, C. A. McLellan, C. Siefe, J. A. Dionne, *ACS Photonics* **2020**, *8*, 3–17.

[9] S. Grabtchak, L. G. Montgomery, W. M. Whelan, *Phys. Med. Biol.* **2014**, *59*, 2431–2444.

[10] O. T. Bruns, T. S. Bischof, D. K. Harris, D. Franke, Y. Shi, L. Riedemann, A. Bartelt, F. B. Jaworski, J. A. Carr, C. J. Rowlands, M. W. B. Wilson, O. Chen, H. Wei, G. W. Hwang, D. M. Montana, I. Coropceanu, O. B. Achorn, J. Kloepper, J. Heeren, P. T. C. So, D. Fukumura, K. F. Jensen, R. K. Jain, M. G. Bawendi, *Nat. Biomed. Eng.* **2017**, *1*, 0056.